RSC Advances

PAPER

View Article Online
View Journal | View Issue

Cite this: *RSC Adv.*, 2022, **12**, 25860

Generation and characterization of coal-based needle coke produced by the co-carbonization of coal liquefaction pitch and anthracene oil

Yuzhu Zhang,[a] Xiang Liu,[b] Miaomiao Tian,[a] Yaming Zhu, *[ac] Chaoshuai Hu[a] and Xuefei Zhao*[a]

In this study, we studied the feasibility of preparing high-quality needle coke from coal liquefaction pitch. Nine types of blending pitch (coal liquefaction pitch and anthracene oil mixed with different ratios) were used as raw materials to generate needle coke *via* the co-carbonization method. Optical microscopy, X-ray diffraction, Raman spectroscopy and scanning electron microscopy were employed to determine the properties (microstructure, distribution of carbon microcrystals, true density and micro-strength) of the needle coke derived by the co-carbonization method. Actually, the co-carbonization of coal liquefaction pitch and anthracene oil was an essential method to control the micro-structure and property of the derived needle coke. Briefly, the needle coke derived by the co-carbonization of coal liquefaction pitch and anthracene oil had a lower content of mosaic structure of 14.17%, ideal carbon crystal content of 82.67%, and true density of 2.296 g cm^{-3}. Briefly, the addition of anthracene oil is a suitable method to adjust the property of coal liquefaction pitch, which is also a good method to produce high-quality needle coke *via* the co-carbonization of coal liquefaction pitch and anthracene oil. Thus, the use of coal liquefaction pitch and anthracene oil as raw materials to generate high-quality needle coke is a considerable method to realize the clean and high value-added utilization of coal liquefaction pitch.

Received 10th June 2022
Accepted 28th August 2022

DOI: 10.1039/d2ra03602a

rsc.li/rsc-advances

1 Introduction

Needle coke is generally accepted as a type of multi-functional carbon material with a low coefficient of thermal expansion (CTE), high true density, low specific surface area and good resistance.[1,2] Generally, needle coke is used as an optimizing material to produce ultra-high power graphite electrodes, high power graphite electrodes, anode materials for lithium ion batteries, electrode materials for supercapacitors, *etc.*[3–5] However, the production of high-quality needle coke requires raw materials with a higher basic property of. Generally, aromatic precursors with a high degree of aromatic condensation, low content of sulfur, lower insolubility in quinoline and good viscosity are suitable to generate high-quality needle coke.[6,7]

It is generally accepted that the property of raw materials is one of the most important factors influencing the quality of the derived needle coke. Actually, the co-carbonization method (using blending pitch as raw materials to produce needle coke) is recognized as a good way to adjust the molecular structure distribution and viscosity, and then enhance the quality of the derived needle coke. Specifically, the molecular structure and viscosity of pitch can be controlled by blending different pitches, and the needle coke produced *via* the co-carbonization method has high quality. For example, Li *et al.*[8] produced high-quality needle coke *via* the co-carbonization of coal tar and biomass tar pitch. Yu *et al.*[9] produced high-quality needle coke (coefficient of thermal expansion value not more than 1.62×10^{-6}/°C) *via* the co-carbonization of ethylene tar and fluid catalytic cracking of decant oil. Tian *et al.*[10] blended medium- and low-temperature pitch and coal-based hydrogenated diesel oil for co-carbonization to produce needle coke. Lin *et al.*[11] adjusted the molecular distribution of pitch by mixing coal tar pitch and bio-asphalt. Cheng *et al.*[12] synthesized needle coke with a coefficient of thermal expansion value (CTE) in the range of 3.2×10^{-6}/°C to 0.3×10^{-6}/°C. Mochida *et al.*[13,14] also produced high-quality needle coke with a low CTE *via* the co-carbonization of petroleum vacuum residue and FCC decant oil.

Coal liquefaction pitch (CLP) is a type of complex organic rich in polycyclic aromatic hydrocarbons,[15,16] which is generally obtained from the extraction of direct coal liquefaction residue.[17,18] The molecules of CLP mainly consist of carbon, then hydrogen and some heteroatoms (such as oxygen, sulfur and nitrogen).[19–21] However, to enhance the efficiency and added value of CLP, researchers have used CLP as a raw material to synthesize mesocarbon microbeads (MCMBs), porous carbon, carbon foam, and needle coke.[22–25] As reported in the

[a]*Institute of Chemical Engineering, University of Science and Technology Liaoning, Anshan 114051, China. E-mail: zhuyaming0504@163.com; zhao_xuefei@sohu.com*
[b]*Ansteel Group Iron and Steel Research Institute, Anshan 114003, China*
[c]*Key Laboratory of Chemical Metallurgy Liaoning Province, University of Science and Technology Liaoning, Anshan 114051, China*

literature,[24,25] CLP has an extremely high softening point, which makes the viscosity of the liquid-phase carbonization system higher. The higher viscosity of the liquid-phase carbonization system is easy to generate "foam coke", which reduces the derived needle coke.[26] Furthermore, the aromatic condensation degree of CLP is very high (Lin *et al.*[27] has reported the average molecule formula as $C_{133}H_{106}O_4N_1$) to produce high-quality needle coke. Specifically, controlling the molecular structure distribution and viscosity of CLP is a suitable method to prepare high-quality needle coke.

Coal liquefaction pitch is a type of complex polycyclic aromatic hydrocarbon with a high molecular weight and viscosity, which is produced *via* the extraction of coal direct liquefaction residue and can be employed as a raw material to produce needle coke in theory.[24,25] However, the high viscosity of coal liquefaction pitch makes it difficult to produce high-quality needle coke *via* direct liquid-phase carbonization. Anthracene oil is a significant aromatic component in the coal tar fraction with a low narrow molecular weight distribution and good viscosity. In theory, the blending of CLP and anthracene oil at a suitable rate is a good means to control the molecular structure and decrease the viscosity of blending pitch. Thus, in this study, the co-carbonization of CLP and anthracene oil (blended in varied ratios) was employed to produce high-quality needle coke. Briefly, polarized microscopy, X-ray diffraction, scanning electron microscopy, and Raman spectroscopy were used to examine the microstructure and distribution of the carbon microcrystals. Also, the true density and micro-strength of each needle coke sample were also studied in this work.

2 Experimental

2.1 Raw materials

Coal liquefaction pitch (CLP) was obtained *via* the extraction-distillation method with the coal direct liquefaction residue as the raw material, and the coking washing oil as the solvent. CLP was obtained from China Shenhua Coal To Liquid and Chemical Co., Ltd, and coking washing oil from Angang Steel Group Co., Ltd. Anthracene oil was purchased from Anshan Xingde Materials Technology Co. Ltd. Toluene and quinoline were obtained from Sinopharm Chemical Reagent Beijing Co., Ltd. Proximate analysis and ultimate analysis are recognized as the common parameters for the characterization of the physical–chemical properties of pitch. The physical–chemical properties of the blending pitches (mixture of CLP and anthracene oil) are shown in Table 1.

As listed in Table 1, with an increase in the content of anthracene oil, the proximate analysis (softening point, toluene insoluble, quinoline insoluble and coking value) obviously decreased. CLP-$A_{160\%}$ had the lowest SP, TI, QI and CV of 36 °C, 8.80%, 0.03% and 47.10%, respectively. This phenomenon can be attributed to the properties of anthracene oil. Anthracene oil is one of the important components in coal tar. Anthracene oil has good mobility, lower aromatic condensation, and extreme insolubility in toluene than CLP. Consequently, the greater the content of anthracene oil in the blending pitch, the lower its proximate analysis.

The additive of anthracene oil had little influence on the content of N and S, but had a great influence on the distribution of H and O. Actually, the additive of anthracene oil had an obvious influence on the C/H ratio ($R_{C/H}$). Briefly, the greater the content of anthracene oil in the blending pitch, the lower its $R_{C/H}$. Actually, CLP had the highest $R_{C/H}$ of 1.42, while CLP-$A_{160\%}$ had the $R_{C/H}$ of 1.31.

2.2 Preparation of needle coke by co-carbonization of CLP and anthracene oil

25 g blending pitch (mixture of CLP and anthracene oil at different ratios) was placed in a neck glass tube. The glass tube was then placed in a pit resistance furnace, and then the pit resistance furnace was heated from room temperature to 500 °C and held for 4 h (the heating rate of 1 °C min^{-1}) for the co-carbonization process. After the co-carbonization process, the green needle coke was obtained. The green needle coke was transferred to a tube-type resistance furnace for calcination. Briefly, the green needle coke was heated to 1400 °C for 1 h at a heating rate of 5 °C min^{-1}, and pure N_2 was used as an inert atmosphere. Needle coke was obtained after the calcination, which was denoted as CLP-A_X-C (X represents the added content of anthracene oil). A flow diagram of the process for the preparation of needle coke is presented in Fig. 1.

Table 1 The physical–chemical of blending pitches

	Proximate analysis					Ultimate analysis/%					
Sample	SP/°C	TI/%	QI/%	CV/%	V/%	C/%	H	N	S	O	$R_{C/H}$
CLP	158	20.58	0.17	66.56	50.21	90.37	5.30	1.05	0.11	3.17	1.42
CLP-$A_{20\%}$	97	18.82	0.16	61.66	53.52	90.08	5.48	1.23	0.19	3.02	1.37
CLP-$A_{40\%}$	89	17.41	0.15	59.91	54.17	90.23	5.45	1.19	0.22	2.91	1.38
CLP-$A_{50\%}$	72	14.72	0.07	60.60	55.79	90.07	5.53	1.17	0.36	2.87	1.36
CLP-$A_{80\%}$	61	14.54	0.06	55.51	57.30	89.90	5.65	1.11	0.50	2.85	1.33
CLP-$A_{100\%}$	58	10.22	0.08	54.32	59.54	89.39	5.75	1.05	0.80	3.02	1.30
CLP-$A_{120\%}$	56	10.90	0.08	53.38	60.98	90.28	5.66	1.08	0.79	2.2	1.33
CLP-$A_{140\%}$	46	9.51	0.06	49.22	63.55	90.29	5.77	1.07	0.69	2.19	1.30
CLP-$A_{160\%}$	36	8.80	0.03	47.10	64.63	90.02	5.72	1.05	0.76	2.47	1.31

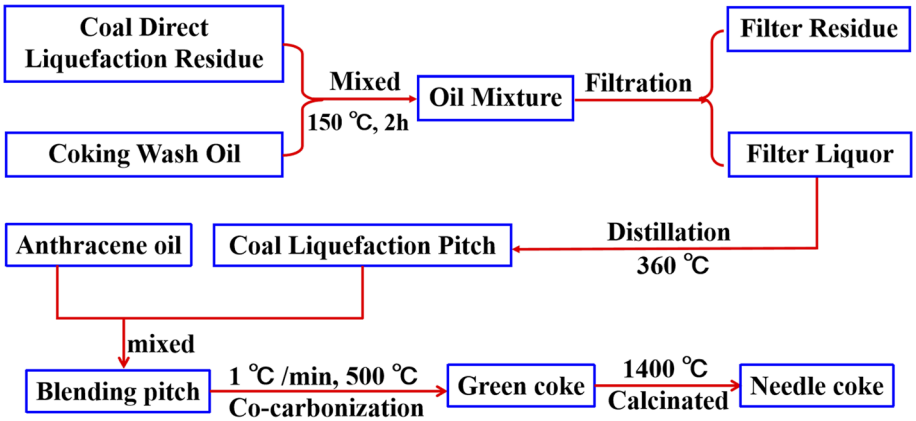

Fig. 1 Flow diagram of the preparation process of needle coke.

2.3 Characterization

2.3.1 Proximate analysis and ultimate analysis of blending pitches. The softening point (SP), coking value (CV), toluene insoluble (TI) and quinoline insoluble (QI) of the pitch were tested according to the literature.[28,29] The element content (C, H, N, and S) distribution was determined using an elemental analyzer (Vario ELIII, Elmentar, German) *via* the combustion method. Actually, the content of O was calculated using the difference method.

2.3.2 FTIR spectrum analysis of blending pitches. CLP is a type of complex compound, where its functional groups have a significant influence on its thermal conversion behavior. FTIR is usually used as an efficient method to judge the molecular structure of pitch. The blending pitches were determined using a NICOLETIS5 FT-IR spectrometer (Thermo Nicolet Corporation, America).

2.3.3 ^{1}H-NMR analysis of blending pitches. An NMR spectrometer (AVANCE III, Bruker, German) was used to examine the aromatic index (f_a) of the blending pitches. Actually, the f_a of the blending pitches was determined using ^{1}H-NMR, with deuterated dimethyl sulfoxide as the solvent. Actually, the hydrogen type of pitch in ^{1}H-NMR is generally classified into H_γ (chemical shift from 0 to 1.0 ppm), H_β (chemical shift from 1.0 ppm to 2.0 ppm), H_α (chemical shift from 2.0 ppm to 4.5 ppm), and H_{ar} (chemical shift from 6.5 ppm to 9.5 ppm). The method for the calculation of f_a was according to the literature,[30–32] and presented as eqn (1), as follows:

$$f_a = \frac{\frac{C}{H} - \frac{(H_\alpha + H_\beta + H_\gamma)}{X}}{\frac{C}{H}} \quad (1)$$

where X means for the ratio of saturated hydrogen to carbon atoms on the aromatic ring, which is usually 2.4 for coal pitch.

2.3.4 Polarized microscopy analysis of needle coke derived from the co-carbonization of CLP and anthracene oil. Polarized microscopy is one of the most important measurements to judge the microstructure of needle coke. Actually, the optical microstructure of coke (including metallurgy coke, pitch coke and needle coke) usually consists of mosaic structures (coarse mosaic structure, medium mosaic structure and fine mosaic structure), fibrous structures (coarse fibrous structures and fine fibrous structures) and leaflet microstructures. The optical microstructure of the needle coke was determined using a polarized microscope (Axio Scope A1 pol, Carl Zeiss, German), and the identification standard of the optical microstructure of the needle coke was according to the literature.[33–35]

2.3.5 XRD analysis of needle coke derived from the co-carbonization of CLP and anthracene oil. The carbon microcrystalline parameters including content of ideal carbon crystal and stacking height of the carbon crystal are generally accepted as a common index to judge the quality of needle coke. Actually, the carbon microcrystal of the needle coke derived by the co-carbonization of CLP and anthracene oil was tested *via* the combination of a powder X-ray diffraction (PANalytical B.V., Netherlands) and the curve-fitting method. The curve-fitting standard was according to our previous studies.[33–35]

2.3.6 Raman spectrum analysis of needle coke derived from the co-carbonization of CLP and anthracene oil. The Raman spectroscopy and curve-fitting method are usually used as a useful method to characterize the distribution of carbon microcrystals. Actually, the carbon microcrystals (determined by the combination of Raman spectroscopy and curve-fitting method) include graphite crystals and amorphous carbon. The Raman spectrum of the needle coke was measured on a Raman spectrometer (LabRAM HR Evolution, JOBIN YVON, France), and the curve-fitting standard was according to our previous research.[33–35]

2.3.7 SEM analysis of needle coke derived from the co-carbonization of CLP and anthracene oil. The morphology of the needle coke derived from the co-carbonization of CLP and anthracene oil was characterized by scanning electron microscopy (∑IGMA-HD, Carl Zeiss, Germany).

2.3.8 Micro-strength and true density of needle coke derived from the co-carbonization of CLP and anthracene oil. The micro-strength and true density of needle cokes derived from the co-carbonization of CLP and anthracene oil were determined using the Ragan and Marsh method[36] and the National Standard of China (GB/T 32158-2015), respectively.

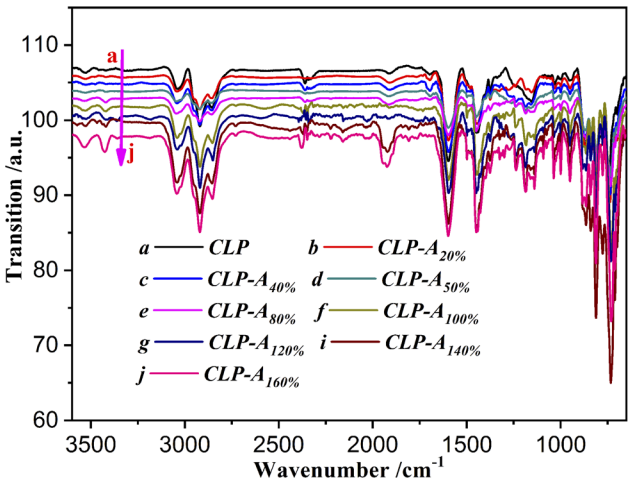

Fig. 2 FTIR spectra of the blending pitches.

3 Results and discussion

3.1 FTIR analysis (molecular structure analysis) of the blending pitches

FTIR was used to determine the molecular structure of the blending pitch. The FTIR spectra are presented in Fig. 2.

As shown in Fig. 2, the absorption peaks were extremely similar in the different blending pitch samples. As listed in the literature,[30–32] the absorption peak at around 3450 cm^{-1} is attributed to the vibration of the –OH functional groups. The vibration of the functional groups of aromatic hydrogen corresponds to the absorption peaks at around 3050 cm^{-1}. The absorption peaks in the range of 2800 cm^{-1} to 3000 cm^{-1} are caused by the vibration of $-CH_3$ and $-CH_2-$. Furthermore, the oxygen-containing functional groups (C═O, C–O, and C═OOH) correspond to the absorption peaks at around 1000–1800 cm^{-1}. Actually, as shown in Fig. 2, the species of functional groups in the blending pitches were similar.

3.2 The aromatic index (f_a) of the blending pitches

In our previous studies,[27] aromatic index (f_a) was one of the key indices reflecting the feasibility of raw pitch to produce high-quality coal-based needle coke. Generally, the refined coal pitch with f_a of 0.95–0.98 was suitable to prepare high-quality needle coke. The method for the calculation of f_a for the raw pitch is according to eqn (1), which is also presented in the literature.[30–32] The ^{1}H-NMR graph of CLP and the distribution of f_a in the series blending pitches are shown in Fig. 3.

As presented in Fig. 3(a–i), the ^{1}H-NMR spectra of the raw pitches can be divided into 4 types, corresponding to the aliphatic hydrogens in methyl or methylene groups in the γ-position to an aromatic ring (H_γ), aliphatic hydrogen in the methyl or methylene groups in the β-position to an aromatic ring (H_β), aliphatic hydrogen in methyl or methylene groups in the α-position to an aromatic ring (H_α) and aromatic hydrogen (H_A), respectively. The f_a of each blending pitches was calculated according to the literature[30–32] and listed in Fig. 3(j). The f_a of the blending pitches is in the range of 0.9507 to 0.9586, which is in the range of 0.95–0.98. Thus, these blending pitches are suitable to generate coal-based needle coke.

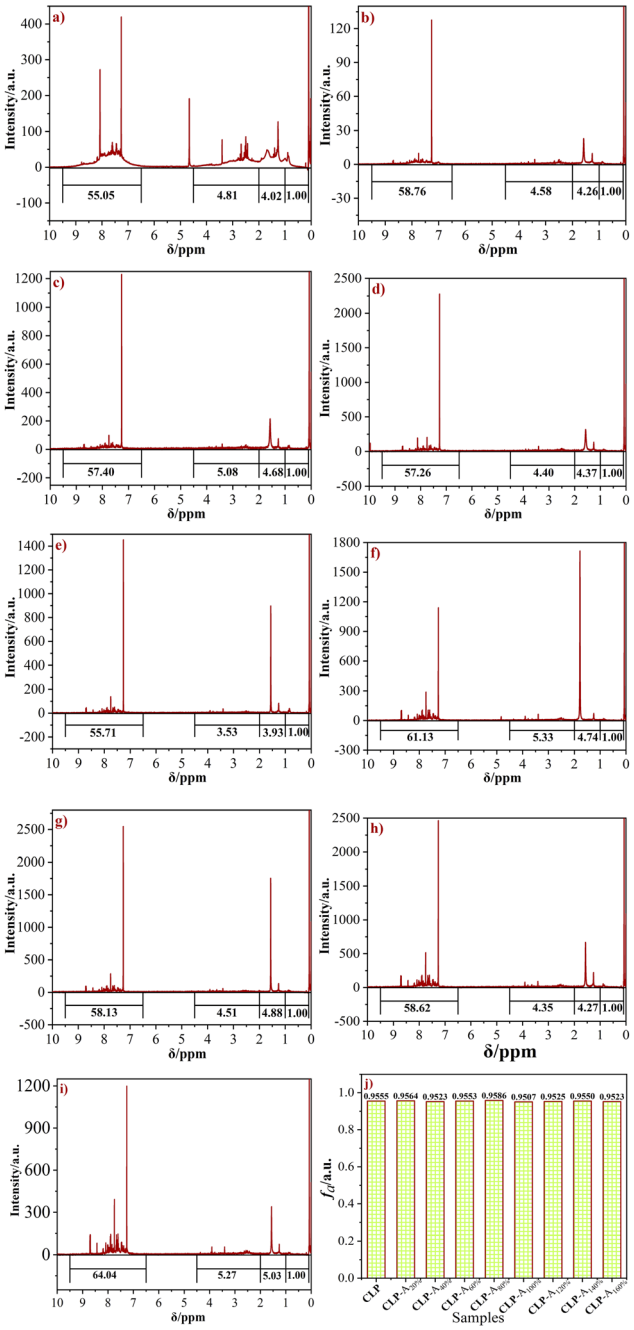

Fig. 3 ^{1}H-NMR spectra of CLP (a), CLP-$A_{20\%}$ (b), CLP-$A_{40\%}$-C (c), CLP-$A_{50\%}$ (d), CLP-$A_{80\%}$ (e), CLP-$A_{100\%}$ (f), CLP-$A_{120\%}$ (g), CLP-$A_{140\%}$ (h), CLP-$A_{160\%}$ (i) and distribution of f_a (j) of raw pitches.

3.3 Preparation of green needle coke from blending pitches

The green needle coke was synthesized using different blending pitches *via* the co-carbonization method. A picture of the green needle coke is shown in Fig. 4.

As shown in Fig. 4, the green needle coke derived from the sole coal liquefaction pitch overflowed at the mouth of the

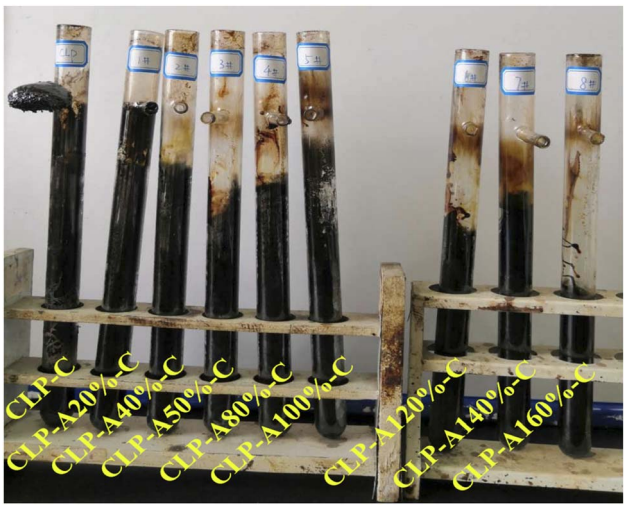

Fig. 4 Optical images of the produced needle coke.

mouth-tube, which is often considered a "foam-like coke phenomenon". This phenomenon is attributed to the extremely reactive nature or ultra-high viscosity of the reaction system during the liquid-phase carbonization process.[37,38] In fact, the coal liquefaction pitch (CLP) was obtained from the coal direct liquefaction residue, and thus the average molecular weight of the CLP was relatively higher than that of the common pitch (such as high-temperature coal tar pitch and medium-low-temperature pitch). Consequently, the reactivity of the pitch molecules in CLP was relatively low. Actually, the softening point and toluene insoluble but quinoline insoluble (β resin) of CLP were 158 °C and 20.41% (listed in Table 1), respectively. Specifically, the "foam-like coke phenomenon" in the needle coke derived from CLP was caused by the high viscosity of the reaction system in the liquid-phase carbonization process.

The green needle coke from the blending pitch of CLP-$A_{20\%}$ reached the mouth of the mouth-tube. The "foam-like coke phenomenon" of CLP-$A_{20\%}$-C was obviously less than that of CLP-C. Furthermore, the more additive of anthracene oil in the blending pitch, the lower the "foam-like coke phenomenon" in the derived green needle coke. This phenomenon can be illustrated by the viscosity of the blending pitches. As listed in Table 1, the SP and TI of the blending pitch obviously decreased with an increase in the content of anthracene oil added (SP and TI of CLP-$A_{160\%}$ were 36 °C and 8.80%, respectively). Consequently, the viscosity of the pitch system during the liquid-phase carbonization process was gradually reduced with an increase in the content of anthracene oil additive. The pyrolysis gas from the blending pitch during the liquid-phase carbonization could escape from the system, and thus the "foam-like coke phenomenon" of the green needle coke disappeared with the addition of anthracene oil.

3.4 Optical microstructure of needle coke derived from blending pitches

Polarized microscopy and the carbon theory are generally accepted as the common and useful method to determine the optical microstructure of needle coke. Generally, the distribution of the optical structure is accepted as one of the key indices to judge the quality of needle coke. Actually, the optical microstructure of the needle coke consisted of mosaic structures (including coarse mosaic structure, medium mosaic structure and fine mosaic structure), fibrous structures (coarse fibrous structure and fine fibrous structure) and leaflet structures.[39] The typical optical microstructure of needle coke derived from blending pitch is presented in Fig. 5.

As reported in the literature,[39] the combination of polarized microscopy and carbon theory is recognized as a suitable method to statistically determine the content of each type of optical microstructure of the needle cokes. Actually, the classified and statistic method was according to the literature, and the effective collection points were more than 500 points to guarantee the accuracy. The distribution of the optical microstructures of the needle coke derived from the different blending pitch samples is listed in Table 2.

As listed in the Table 2, the content of mosaic structure in CLP-C was 26.15%, which is the highest among the needle cokes derived from the co-carbonization of CLP and anthracene oil. In fact, the mosaic structure in needle coke is recognized as the component that is difficult to undergo graphitization during graphitization treatment. Specifically, a lower content of mosaic structure in needle coke indicates a good graphitization property. Actually, the pitch coke with a content of mosaic structure lower than 24% can be classed as needle coke, where the lower content of mosaic structure indicates the good quality of the needle coke. As presented in Table 2, the content of mosaic structure gradually decreased with an increase in the ratio of the additive anthracene oil. This phenomenon can be attributed to the good viscosity of the blending pitches. In fact, the greater the ratio of anthracene oil, the lower the SP and TI in the blending pitches. A lower SP and TI always indicate a lower viscosity of the blending pitch. With an increase in the liquid-phase carbonization temperature, the mobility of the pitch is enhanced. Consequently, the pyrolysis gas during the co-carbonization process easily escapes from the system in the same direction. Furthermore, the escape of the pyrolysis gas may promote the formation of a "domain-type mesophase" during the liquid-phase carbonization process. Thus, the content of mosaic structure obviously decreased with an increase in the content of anthracene oil.

3.5 The carbon microcrystalline of needle coke from X-ray diffraction

X-ray diffraction is usually used to characterize the carbon microcrystalline of needle coke. Generally, the combination of XRD and the curve-fitting method is recognized as a suitable method for the quantitative analysis of the carbon microcrystalline of needle coke. The XRD graph and curve-fitting curve of the needle cokes are shown in Fig. 6.

As presented in Fig. 6(a), the asymmetrically broad peak at around 26° is the typical characteristic peak of the ungraphitized carbon, which is also called the (002) peak. The diffraction position and shape of the (002) peak are similar for the series of needle cokes, but the intensity and width of the (002) peak

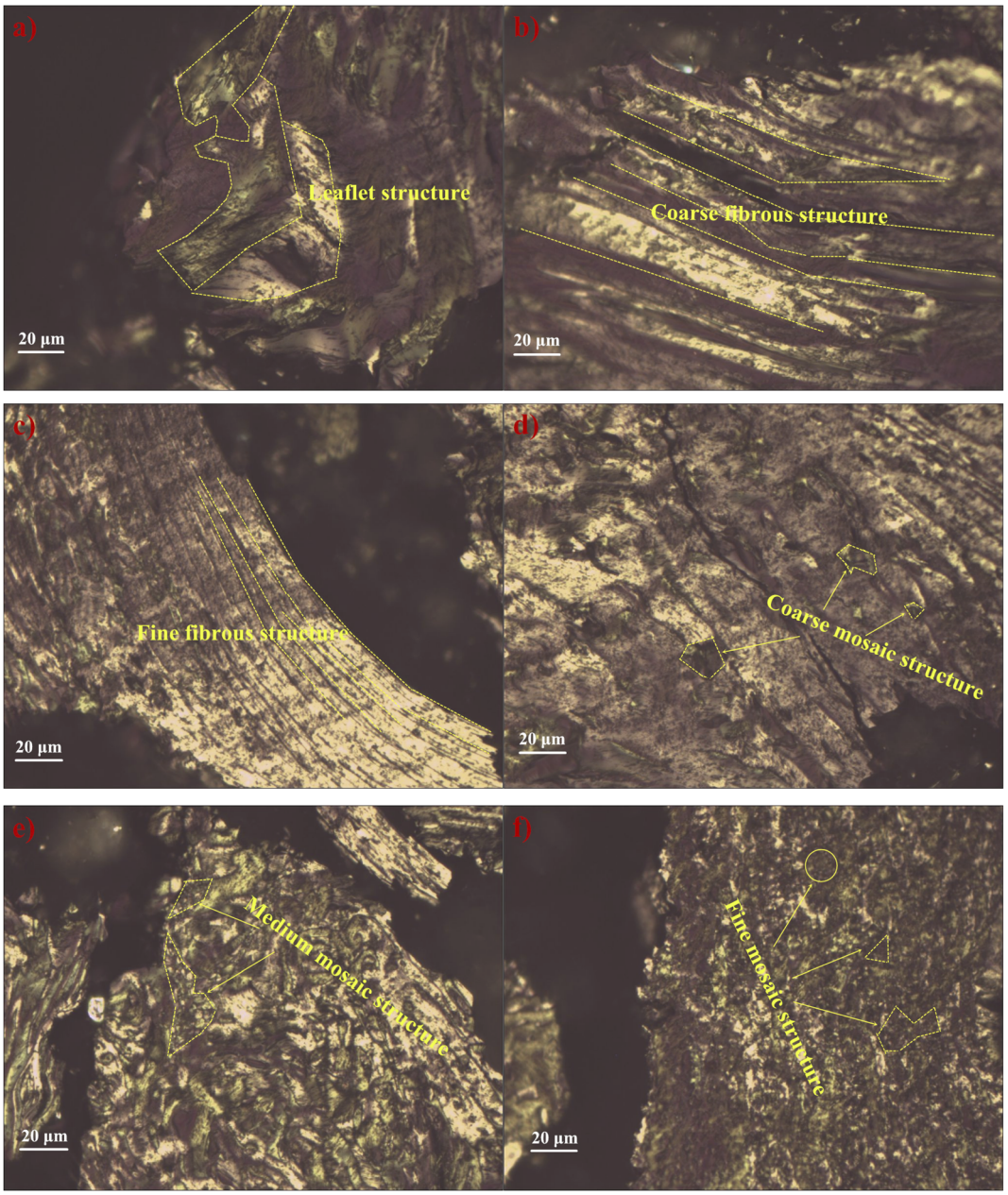

Fig. 5 Typical optical microstructure of needle cokes: leaflet structure (a), coarse fibrous structure (b), fine fibrous structure (c), coarse mosaic structure (d), medium coarse structure (e), and fine mosaic structure (f).

Table 2 Distribution of the optical microstructure of the needle coke

	Optical microstructure/%			
Sample	Mosaic structure	Coarse fibrous	Fine fibrous	Leaflet structure
CLP-C	26.15	0.77	31.54	41.54
CLP-$A_{20\%}$-C	20.66	3.31	37.19	38.84
CLP-$A_{40\%}$-C	24.80	0.80	40.80	33.60
CLP-$A_{50\%}$-C	22.67	1.33	32.67	43.33
CLP-$A_{80\%}$-C	17.35	2.04	29.59	51.02
CLP-$A_{100\%}$-C	16.92	1.54	40.00	41.54
CLP-$A_{120\%}$-C	20.67	1.48	41.48	36.37
CLP-$A_{140\%}$-C	20.37	2.78	40.74	36.11
CLP-$A_{160\%}$-C	14.17	3.32	45.84	36.67

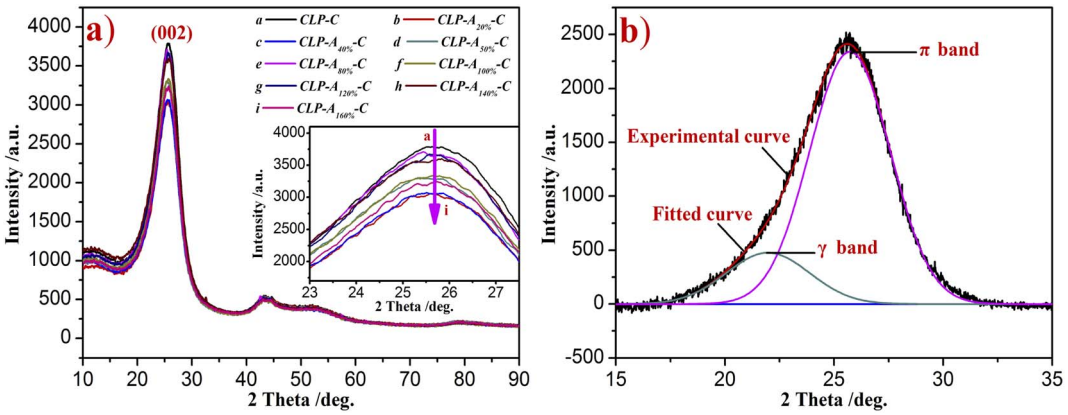

Fig. 6 XRD patterns of needle coke (a) and curve-fitted graph of CLP-$A_{20\%}$-C (b) 0.

obviously varied for each sample. Actually, the higher intensity and narrower width of the (002) peak indicate the regular carbon microcrystalline structure of the needle coke. As reported in the literature,[40] the carbon microcrystalline parameters of needle coke can be determined by the combination of XRD and the curve-fitting method.

Generally, the (002) peak consisted of two symmetric peaks at around 22° and 26°, which are called the γ-band and π-band, respectively. The peak area and 2θ value of the π-band are the key data to calculate the parameters including Ig, Lc, N and n. Briefly, Ig represents the content of ideal graphite carbon and Lc is the lateral size of the needle coke. N and n represent parallel layers and average number of aromatic rings in each layer, respectively. The formula employed for the calculation was also according to the literature,[33–35] and the carbon microcrystalline parameters of the needle cokes derived from the liquid-phase carbonization of the blending pitches are shown in Table 3.

As listed in Table 3, the Ig of CLP-C was 77.07%, which was the lowest in the needle coke series. However, CLP-$A_{160\%}$-C had the highest Ig of 80.55%. In fact, the Ig of the derived needle cokes obviously increased with an increase in the additive ratio of anthracene oil in the blending pitches. The structural parameters of Lc, N and n in the needle coke series showed a similar trend to Ig. Actually, the Lc, N and n of the derived

Table 3 The structural parameters of the needle coke samples

Sample	γ/°	π/°	A_γ	A_π	I_g/%	L_c/nm	N	n
CLP-C	22.03406	25.72793	2701.31	9078.40	77.07	1.91	8.27	21.87
CLP-$A_{20\%}$-C	21.97285	25.72844	1600.66	7594.39	82.59	1.91	8.29	22.01
CLP-$A_{40\%}$-C	22.15738	25.73790	1882.24	7366.06	79.65	1.92	8.42	22.67
CLP-$A_{50\%}$-C	21.82827	25.72893	1687.09	8354.93	83.20	1.95	8.43	22.74
CLP-$A_{80\%}$-C	22.09054	25.73165	2175.66	9076.78	80.66	1.93	8.40	22.60
CLP-$A_{100\%}$-C	21.98202	25.73290	1947.82	8322.01	81.03	1.92	8.37	22.42
CLP-$A_{120\%}$-C	22.16178	25.76571	2228.54	8867.26	79.92	1.92	8.75	24.47
CLP-$A_{140\%}$-C	21.99676	25.75850	2003.26	9049.48	81.88	1.93	8.72	24.33
CLP-$A_{160\%}$-C	22.00506	25.748540	1676.13	7997.58	82.67	1.96	8.72	24.33

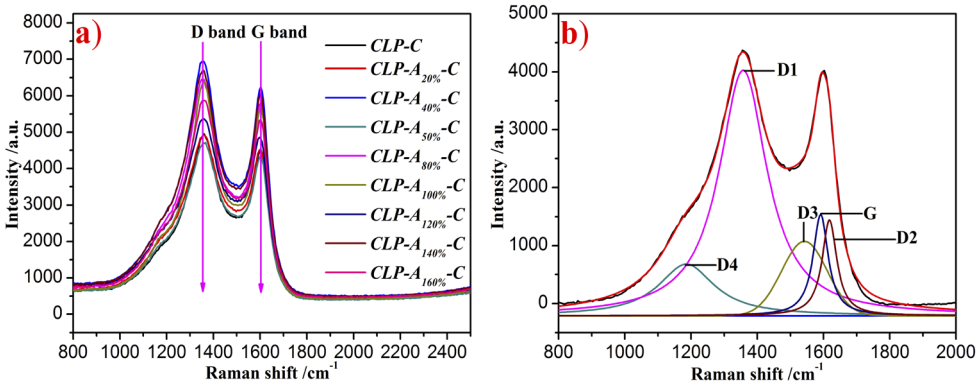

Fig. 7 Raman spectra of needle cokes (a) and curve-fitted graph of CLP-$A_{20\%}$-C (b).

needle cokes were in the range of 1.91–1.96 nm, 8.27–8.72, and 21.87–24.33, respectively. Obviously, the CLP-C and CLP-$A_{160\%}$-C presented as the endpoint data (the CLP-C has the lowest point and CLP-$A_{160\%}$-C has the highest point). This phenomenon can be illustrated by the physical–chemical property of the blending pitch, especially the viscosity of the blending pitch. As reported in the literature, due to the lower viscosity and good mobility of the raw pitch during the liquid-phase carbonization process, it was easier to generate a "domain mesophase" structure in the needle coke. Consequently, the carbon microcrystalline structure of the derived needle coke with a greater ratio of anthracene oil in the blending pitch was more regular, which is consistent with the optical microstructure of the needle coke.

3.6 Distribution of carbon microcrystalline of needle coke from Raman spectroscopy

Raman spectroscopy is also accepted as a practical method to judge the distribution of carbon microcrystalline structure in needle coke. The Raman spectra of the needle coke series are shown in Fig. 7.

As shown in Fig. 7(a), there were two obvious "hump pattern" peaks at around 1360 cm^{-1} and 1580 cm^{-1}, which were denoted as the "D" band and "G" band, respectively. These two typical peaks are the characteristic peaks of ungraphitized carbon materials and caused by the vibration of disordered carbon and ideal carbon crystals, respectively. However, the intensity and width of the vibration peaks in each needle coke sample were mixed, making it difficult to judge the distribution of the carbon microcrystalline structure in each needle coke sample.

As reported in the literature,[41] the "hump pattern" peaks of the needle cokes consisted of 5 isolated symmetrical peaks, which were named as the D1 band, D2 band, D3 band, D4 band and G band. Briefly, the D3 band was caused by the vibration of amorphous carbon and the G band is ascribed to the ideal carbon crystal (also called graphite carbon crystal). Furthermore, the D1 band, D2 band and D4 band are attributed to the defective carbon microcrystalline structures (these types of carbon microcrystalline structures easily undergo graphitization at the graphitization temperature). The Raman spectrum of each needle coke was curve-fitted into 5 isolated peaks (Fig. 7(b)) according to the literature,[35] and the distribution of the carbon microcrystalline structures of each needle coke is listed in Table 4 (the parameters were calculated using the peak area).

As shown in Table 4, I_G/I_{All} and I_{D3}/I_{All} correspond to the content of graphite carbon and content of amorphous carbon in the needle coke, respectively. CLP-C had the lowest I_G/I_{All} of 7.78%, whereas CLP-$A_{160\%}$-C had the highest I_G/I_{All} of 10.42%. Specifically, the content of graphite carbon obviously increased with an increase in the content of anthracene oil additive. On the contrary, the I_{D3}/I_{All} of CLP-C, CLP-$A_{20\%}$-C, CLP-$A_{40\%}$-C, CLP-$A_{50\%}$-C, CLP-$A_{80\%}$-C, CLP-$A_{100\%}$-C, CLP-$A_{120\%}$-C, CLP-$A_{140\%}$-C and CLP-$A_{160\%}$-C was 12.12%, 11.45%, 11.81%, 11.64%, 11.77%, 11.61%, 11.71%, 11.57% and 11.45%, respectively. Specifically, the content of amorphous carbon gradually decreased with an increase in the ratio of anthracene oil additive in the derived needle coke. Furthermore, the distribution of carbon microcrystalline structures in the derived needle coke was consistent with the results of the optical microstructure and XRD analysis, and the distribution of I_G/I_{All} and I_{D3}/I_{All} in the needle coke series showed the opposite data trend.

3.7 Morphology of needle coke from Raman spectroscopy

Needle coke is a type of graphitized carbon material, which has a dominant morphology of graphitic structure. Scanning electron microscopy (SEM) was used as an important tool to investigate the morphology of the needle coke, and the SEM images of each needle coke are shown in Fig. 8.

As presented in Fig. 8, the morphology of CLP-C was dominantly a graphitic lamellar structure but some mosaic structures were also present, as shown in Fig. 7(a). The morphology of the needle cokes derived from the co-carbonization of CLP and anthracene oil was dominantly fibrous structure, graphitic lamellar structure and leaflet structure, and hardly any defect structures or mosaic structures were observed. Specifically, the mosaic structure in the co-carbonization needle cokes was less than that in CLP-C, and this result is consistent with the results from the optical microstructure. Actually, the anthracene oil additive may reduce the viscosity of the reaction system during the liquid-phase carbonization process. Thus, the pyrolysis gas could escape smoothly from the system in a same direction. Consequently, due to the microstructure of the needle coke, it was easier to generate a fibrous structure during the latter stage

Table 4 Curve-fitting data of the needle coke samples

	Integrate area					Ratio/%	
Sample	I_{D1}	I_{D2}	I_{D3}	I_{D4}	I_G	I_G/I_{All}	I_{D3}/I_{All}
CLP-C	675 420	98 322	138 619	142 494	88 948	7.78	12.12
CLP-$A_{20\%}$-C	782 165	102 160	150 134	170 625	106 047	8.09	11.45
CLP-$A_{40\%}$-C	710 236	90 912	143 106	168 297	99 033	8.17	11.81
CLP-$A_{50\%}$-C	808 245	113 960	161 664	189 100	116 092	8.36	11.64
CLP-$A_{80\%}$-C	672 992	79 487	135 318	163 151	98 571	8.57	11.77
CLP-$A_{100\%}$-C	886 624	116 378	180 648	225 873	145 923	9.38	11.61
CLP-$A_{120\%}$-C	839 827	110 657	173 313	212 997	143 660	9.70	11.71
CLP-$A_{140\%}$-C	902 294	122 647	183 876	224 919	155 142	9.76	11.57
CLP-$A_{160\%}$-C	780 667	109 105	157 174	183 123	143 059	10.42	11.45

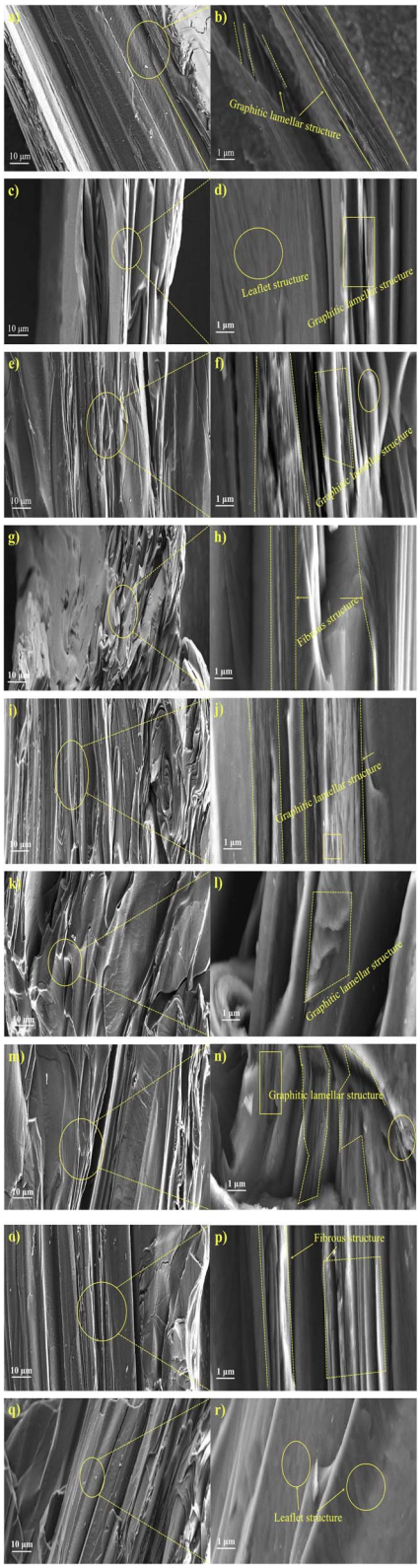

Fig. 8 SEM images of needle coke: (a and b) CLP-C, (c and d) CLP-$A_{20\%}$-C, (e and f) CLP-$A_{40\%}$-C, (g and h) CLP-$A_{50\%}$-C, (i and j) CLP-$A_{80\%}$-C, (k and l) CLP-$A_{100\%}$-C, (m and n) CLP-$A_{120\%}$-C, (o and p) CLP-$A_{140\%}$-C, and (q and r) CLP-$A_{160\%}$-C.

Table 5 Micro-strength of needle coke samples

Sample	Micro-strength/%
CLP-C	70.0%
CLP-$A_{20\%}$-C	63.3%
CLP-$A_{40\%}$-C	64.5%
CLP-$A_{50\%}$-C	63.8%
CLP-$A_{80\%}$-C	62.1%
CLP-$A_{100\%}$-C	65.0%
CLP-$A_{120\%}$-C	61.9%
CLP-$A_{140\%}$-C	65.4%
CLP-$A_{160\%}$-C	63.7%

of the carbonization process. Specifically, the co-carbonization of CLP and anthracene oil is a good method to enhance the quality of the derived needle coke.

3.8 Micro-strength of needle coke

Micro-strength is usually used to judge the strength of the carbon skeleton of needle coke. The micro-strength of the needle coke samples is listed in Table 5.

As listed in Table 5, CLP-C had the highest micro-strength of 70.0%, whereas the micro-strength of the other needle coke samples derived from the blending pitches was lower than 70% but higher than 61%. According to the literature,[42] the mosaic structures (coarse mosaic, medium mosaic and fine mosaic) in coke contribute more to the micro-strength than fibrous structures or leaflet structures. Actually, the fibrous structure or leaflet structure has a higher orientation degree than the mosaic structures. The mosaic structure in the needle coke was observed to exhibit optical anisotropy but macroscopic isotropy. Consequently, the greater content of mosaic structure, the higher the micro-strength. The strength of the carbon skeleton has an important influence on the property of the derived carbon materials, and thus the needle cokes with a micro-strength higher than 61% can be considered as high-quality needle cokes.

3.9 True density of needle cokes

True density is recognized as a key parameter to judge the quality of the needle coke. Actually, the needle cokes used as raw materials to produce ultra-high graphite electrodes require a true density of higher than 2.10 g cm^{-3} at the calcination

Table 6 True density of needle coke samples

Sample	ρ_T/g cm^{-3}
CLP-C	1.867
CLP-$A_{20\%}$-C	1.958
CLP-$A_{40\%}$-C	1.986
CLP-$A_{50\%}$-C	1.988
CLP-$A_{80\%}$-C	2.021
CLP-$A_{100\%}$-C	2.070
CLP-$A_{120\%}$-C	2.180
CLP-$A_{140\%}$-C	2.240
CLP-$A_{160\%}$-C	2.296

temperature of 1450 °C.[42–44] Obviously, a higher calcination temperature always results in a higher true density of needle coke. The true density of the needle coke derived from the blending pitches is listed in Table 6.

As listed in Table 6, CLP-C had the lowest true density of 1.867 g cm^{-3}. The true density of CLP-$A_{20\%}$-C, CLP-$A_{40\%}$-C, CLP-$A_{50\%}$-C, CLP-$A_{80\%}$-C, CLP-$A_{100\%}$-C, CLP-$A_{120\%}$-C, CLP-$A_{140\%}$-C and CLP-$A_{160\%}$-C was 1.958 g cm^{-3}, 1.986 g cm^{-3}, 1.988 g cm^{-3}, 2.021 g cm^{-3}, 2.070 g cm^{-3}, 2.180 g cm^{-3}, 2.240 g cm^{-3} and 2.296 g cm^{-3}, respectively. Specifically, the co-carbonization of CLP and anthracene oil is an essential method to enhance the true density of needle coke. In fact, the needle coke with a lower content of mosaic structure possesses a higher true density. The content of mosaic structures in the co-carbonization needle coke was much lower than that in CLP-C. Consequently, CLP-$A_{160\%}$-C had the highest true density of 2.296 g cm^{-3}, which is in the range of high-quality needle coke according to the literature.[44,45]

4 Conclusions

A series of needle coke samples was produced *via* the co-carbonization of coal liquefaction pitch and anthracene oil. The addition of the anthracene oil had a significant effect on the viscosity and mobility of the blending pitch during the liquid-phase carbonization process. The microstructure (including optical microstructure and carbon microcrystalline structure), micro-strength and true density were used as factors to judge the quality of the derived needle coke employing polarized microscopy, XRD and Raman spectroscopy, respectively. Accordingly, the co-carbonization of CLP and anthracene oil (mixture of CLP and anthracene oil at a suitable ratio) was a good method to produce high-quality needle coke. In fact, the content of fibrous structure and leaflet structure in derived needle coke with the co-carbonization of CLP and anthracene oil reached 85.83%, the content of graphite carbon was 10.42% and the true density was as high as 2.296 g cm^{-3}. Thus, the co-carbonization of CLP and a moderate ratio of anthracene oil are a good method to generate high-quality coal-based needle coke.

Conflicts of interest

The authors declare that there is no conflict of interest regarding the publication of this paper.

Acknowledgements

This work was partially supported by the National Natural Science Foundation of China (U1361126), the Nature Science Foundation of Liaoning Province (2021-MS-306), Foundation of State Key Laboratory of High-efficiency Utilization of Coal and Green Chemical Engineering (2022-K41), Liaoning Provincial Department of Education Project (2020LNQN03), the Excellent Talents Training Program of University of Science and Technology Liaoning (2018RC07).

References

1 Y. L. Guo, Y. M. Li, N. N. Ran and F. Gao, Preparation of mesophase pitch from coliquefaction residue under pressure, *Energy Sources, Part A*, 2016, **38**(18), 2643–2648.
2 H. Hu and M. B. Wu, Heavy oil-derived carbon for energy storage applications, *J. Mater. Chem. A*, 2020, **8**, 7066–7082.
3 Z. H. Ma, X. Y. Wei, G. H. Liu, F. J. Liu and Z. M. Zong, Value-added utilization of high-temperature coal tar: A review, *Fuel*, 2021, **292**, 119954.
4 T. D. Moon, Design integrates delayed coking, needle coke production processes, *Oil Gas J.*, 2021, **119**(9), 84–86.
5 X. J. He, X. J. Li, H. Ma, J. F. Han, H. Zhang, C. Yu, N. Xiao and J. S. Qiu, ZnO template strategy for the synthesis of 3D interconnected graphene nanocapsules from coal tar pitch as supercapacitor electrode materials, *J. Power Sources*, 2017, **340**, 183–191.
6 M. Y. Hao, N. Xiao, Y. W. Wang, H. Q. Li, Y. Zhou, C. Liu and J. S. Qiu, Pitch-derived N-doped porous carbon nanosheets with expanded interlayer distance as high-performance sodium-ion battery anodes, *Fuel Process. Technol.*, 2018, **177**, 328–335.
7 S. A. Dong, X. J. He, H. F. Zhang, X. Y. Xie, M. X. Yu, C. Yu, N. Xiao and J. S. Qiu, Surface modification of biomass-derived hard carbon by grafting porous carbon nanosheets for high-performance supercapacitors, *J. Mater. Chem. A*, 2018, **6**, 15954–15960.
8 L. Li, X. C. Lin, Y. K. Zhang, J. Z. Dai, D. P. Xu and Y. G. Wang, Characteristics of the mesophase and needle coke derived from the blended coal tar and biomass tar pitch, *J. Anal. Appl. Pyrolysis*, 2020, **150**, 104889.
9 Y. Y. Yu, F. Wang, B. W. Biney, K. Q. Li, S. H. Jiao, K. Chen, H. Liu and A. J. Guo, Co-carbonization of ethylene tar and fluid catalytic cracking decant oil: development of high-quality needle coke feedstock, *Fuel*, 2022, **322**, 124170.
10 Y. C. Tian, Y. Huang, X. L. Yu, F. Gao, S. H. Gao, F. L. Wang, D. Li, X. Xu, L. W. Cui, X. Y. Fan, H. Dong and J. Liu, Co-carbonization of medium- and low-temperature coal tar pitch and coal-based hydrogenated diesel oil prepare mesophase pitch for needle coke precursor, *Adv. Eng. Mater.*, 2021, **23**(10), 2001523.
11 X. C. Lin, Z. Sheng, J. He, X. He, C. H. Wang, X. H. Gu and Y. G. Wang, Preparation of isotropic spinnable pitch with high-spinnability by co-carbonization of coal tar pitch and bio-asphalt, *Fuel*, 2021, **295**, 120627.
12 X. L. Cheng, Q. F. Zha, J. T. Zhong and X. J. Yang, Needle coke formation derived from co-carbonization of ethylene tar pitch and polystyrene, *Fuel*, 2009, **88**, 2188–2192.
13 I. Mochida, Y. Korai, T. Oyama, Y. Nesumi and Y. Todo, Carbonization in the tube bomb leading to needle coke: 1. cocarbonization of a petroleum vacuum residue and a FCC decant oil into better needle coke, *Carbon*, 1989, **27**(3), 359–365.
14 I. Mochida, T. Oyama, Y. Q. Fei, T. Furuno and Y. Korai, Optimization of carbonization conditions for needle coke

production from a low-sulphur petroleum vacuum residue, *J. Mater. Sci.*, 1988, **23**, 298–304.

15 J. B. Zhang, L. J. Jin, J. Cheng and H. Q. Hu, Preparation and applications of hierarchical porous carbons from direct coal liquefaction residue, *Fuel*, 2013, **109**, 2–8.

16 J. B. Zhang, L. J. Jin, S. B. Liu, Y. X. Xun and H. Q. Hu, Mesoporous carbon prepared from direct coal liquefaction residue for methane decomposition, *Carbon*, 2012, **50**, 952–959.

17 D. M. Lv, Z. Q. Bai, W. Yuchi, J. Bai, L. X. Kong, Z. X. Guo, X. Li, J. L. Xu and W. Li, Properties of direct coal liquefaction residue water slurry: Effect of treatment by low temperature pyrolysis, *Fuel*, 2016, **179**, 135–140.

18 J. L. Xu, Z. Q. Bai, J. Bai, L. X. Kong, D. M. Lv, Y. N. Han, X. Dai and W. Li, Physico-chemical structure and combustion properties of chars derived from co-pyrolysis of lignite with direct coal liquefaction residue, *Fuel*, 2017, **187**, 103–110.

19 W. Li, Z. Q. Bai, J. Bai and X. Li, Transformation and roles of inherent mineral matter in direct coal liquefaction: A mini-review, *Fuel*, 2017, **197**, 209–216.

20 Y. G. Wang, Z. S. Niu, J. Shen, L. Bai, Y. X. Niu, X. Y. Wei, R. F. Li, J. Zhang and W. Y. Zou, Extraction of direct coal liquefaction residue using dipropylamine as a CO2-triggered switchable solvent, *Fuel Process. Technol.*, 2017, **159**, 27–30.

21 J. B. Zhang, L. J. Jin, S. W. Zhu and H. Q. Hu, Preparation of mesoporous activated carbons from coal liquefaction residue for methane decomposition, *J. Nat. Gas Chem.*, 2012, **21**, 759–766.

22 B. F. Yan and G. Y. Wang, Mechanisms and characteristics of mesocarbon microbeads prepared by co-carbonization of coal tar pitch and direct coal liquefaction residue, *Int. J. Coal Sci. Technol.*, 2019, **6**(4), 633–642.

23 X. L. Cheng, G. N. Li, Y. L. Peng, S. L. Song, X. X. Shi, J. J. Wu, J. X. Xie, M. Zhou and G. Z. Hu, Obtaining needle coke from coal liquefaction residue, *Chem. Technol. Fuels Oils*, 2012, **48**(5), 349–355.

24 Y. Zhou, X. N. Song, C. Shu and J. S. Qiu, The electrochemical properties of templated and activated mesoporous carbons produced from coal pitch, *New Carbon Mater.*, 2011, **26**(3), 187–191.

25 Y. M. Zhu, X. F. Zhao, J. Yuan, C. L. Zhao and C. S. Hu, Changes in structure of coal liquefied pitch during liquid-phase carbonization process, *Carbon Lett.*, 2019, **29**(1), 37–45.

26 Z. H. Chen, Y. Q. Wu, S. Huang, S. Y. Wu and J. S. Gao, Coking behavior and mechanism of direct coal liquefaction residue in coking of coal blending, *Fuel*, 2020, **208**, 118488.

27 H. L. Lin, K. J. Li, X. W. Zhang, H. X. Wang and S. F. Cheng, Analysis and structural model of coal liquefaction asphaltene, *J. Fuel Chem. Technol.*, 2014, **42**(7), 779–783.

28 Y. M. Zhu, S. S. Sun, Y. L. Xu, C. L. Zhao, C. S. Hu, J. X. Cheng and X. F. Zhao, Preparation and characterization of pitch coke from oxidized polymerized pitch, *Asia-Pac. J. Chem. Eng.*, 2020, e2497.

29 Y. M. Zhu, Y. L. Xu, C. S. Hu, X. T. Yin, C. L. Zhao, L. J. Gao and X. F. Zhao, Preparation and characterization of mosaic coke from heavy-phase coal pitch, *Asia-Pac. J. Chem. Eng.*, 2019, e2369.

30 L. J. Gao, X. F. Zhao, S. Q. Lai, J. X. Cheng and Y. Q. Lu, Compositions and Structure Characterizations of Coal Tar Refined Soft Pitch, *Spectrosc. Spectral Anal.*, 2009, **29**(8), 2152–2156.

31 V. Gargiulo, B. Apicella, M. Alfè, C. Russo, F. Stanzione, A. Tregrossi, A. Amoresano, M. Millan and A. Ciajolo, Structural Characterization of Large Polycyclic Aromatic Hydrocarbons. Part 1: The Case of Coal Tar Pitch and Naphthalene-Derived Pitch, *Energy Fuels*, 2015, **29**(9), 5714–5722.

32 V. Gargiulo, B. Apicella, F. Stanzione, A. Tregrossi, M. Millan, A. Ciajolo and C. Russo, Structural Characterization of Large Polycyclic Aromatic Hydrocarbons. Part 2: Solvent-Separated Fractions of Coal Tar Pitch and Naphthalene-Derived Pitch, *Energy Fuels*, 2016, **30**(4), 2574–2583.

33 Y. M. Zhu, C. L. Zhao, Y. L. Xu, C. S. Hu and X. F. Zhao, Preparation and characterization of coal pitch-based needle coke (Part I): the effects of aromatic index (fa) in refined coal pitch, *Energy Fuels*, 2019, **33**, 3456–3464.

34 Y. M. Zhu, C. S. Hu, Y. L. Xu, C. L. Zhao, X. T. Yin and X. F. Zhao, Preparation and characterization of coal pitch-based needle coke (PartII): the effects of β resin in refined coal pitch, *Energy Fuels*, 2020, **34**, 2126–2134.

35 Y. M. Zhu, H. M. Liu, Y. L. Xu, C. S. Hu, C. L. Zhao, J. X. Cheng, X. X. Chen and X. F. Zhao, Preparation and characterization of coal pitch-based needle coke (Part III): the effects of quinoline insoluble in coal tar pitch, *Energy Fuels*, 2020, **34**, 8676–8684.

36 K. Naito, Tensile properties of polyacrylonitrile- and pitch-based hybrid carbon fiber/polyimide composites with some nanoparticles in the matrix, *J. Mater. Sci.*, 2013, **48**, 4163–4176.

37 Z. Zhang, B. Lou, N. Zhao, E. Yu, Z. Wang, H. Du, Z. Chen and D. Liu, Co-carbonization behavior of the blended heavy oil and low temperature coal tar for the preparation of needle coke, *Fuel*, 2021, **302**, 121139.

38 J. M. Wei, S. Z. Zhang, Y. Sheng, X. Y. Gong and C. Chen, Super hard asphalt (SHA) from direct coal liquefaction process as pavement material, *J. Cleaner Prod.*, 2020, **274**, 123815.

39 S. A. Qian, X. Z. Song, R. L. Fan and C. F. Li, The microstructural characteristics of needle cokes-new concept on evaluation of needle coke properties, *J. Fuel Chem. Technol.*, 1981, **9**(2), 105–122.

40 Z. Zhang and Q. Wang, The new method of XRD measurement of the degree of disorder for anode coke material, *Crystals*, 2017, **7**(1), 5.

41 A. Sadezky, H. Muckenhuber, H. Grothe, R. Niessner and U. Pöschol, Raman micro spectroscopy of soot and related

carbonaceous materials: Spectral analysis and structural information, *Carbon*, 2005, **43**, 1731–1742.

42 C. Y. Wang, M. M. Chen and M. W. Li, *Pitch-based carbon materials*, Beijing, Chemical Industry Press, 2018.

43 L. C. Guo, L. E. Jin, C. G. Zhong, Y. Wang and Q. Cao, Effects of a dioctyl phthalate addition to coal tar pitch on the microstructures and electrochemical properties of derived semi-cokes, *New Carbon Mater.*, 2017, **32**(1), 71–76.

44 J. Lv, H. T. Bai, Y. M. Zhu, C. S. Hu, Y. L. Xu, S. Q. Lai and X. F. Zhao, Synthesis and characterization of mesophase coke from medium-low-temperature coal tar pitch modified by high-pressure thermal polymerization, *Asia-Pac. J. Chem. Eng.*, 2021, **16**(4), e2643.

45 Y. M. Zhu, S. S. Sun, Y. L. Xu, C. L. Zhao, C. S. Hu, J. X. Cheng and X. F. Zhao, Preparation and characterization of pitch coke from oxidized polymerized pitch, *Asia-Pac. J. Chem. Eng.*, 2020, **15**(5), e2497.